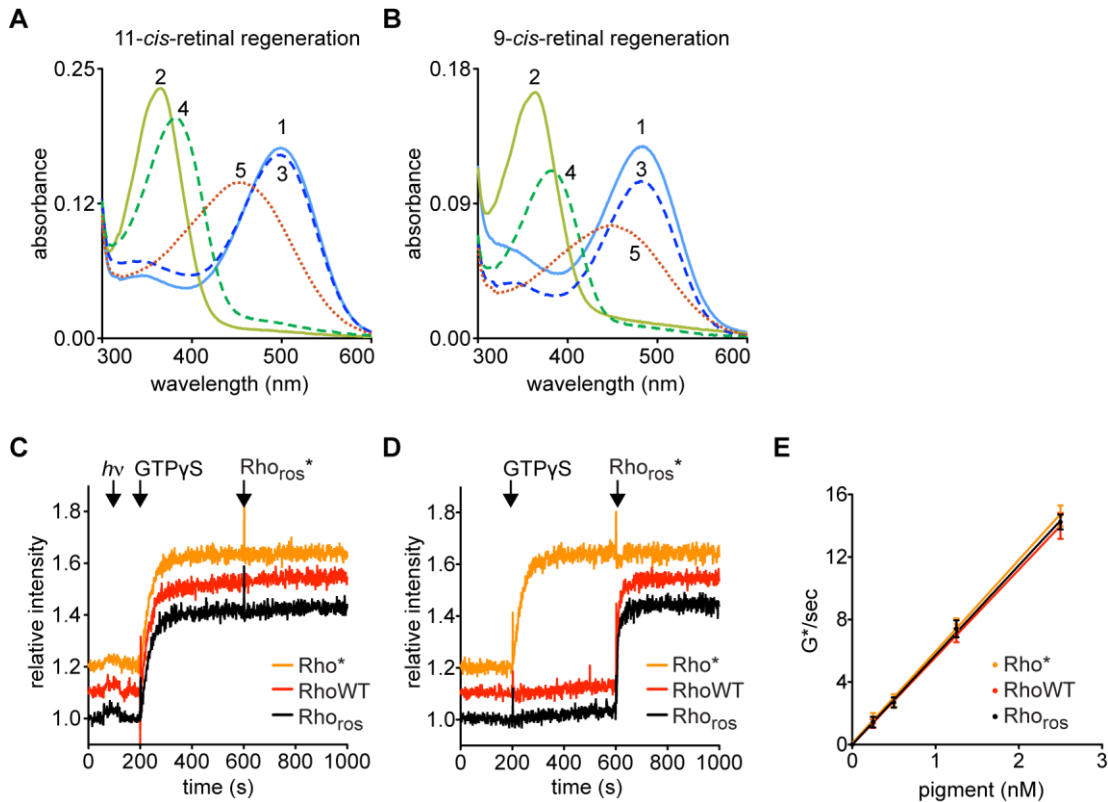


Supplementary Figures



Supplementary Figure 1. Characterization of thermostable opsin and rhodopsins.

The spectroscopic analyses and activity assays shown indicate that the thermostable rhodopsin constructs used in this paper are fully functional vis-à-vis photoactivation and G protein activation.

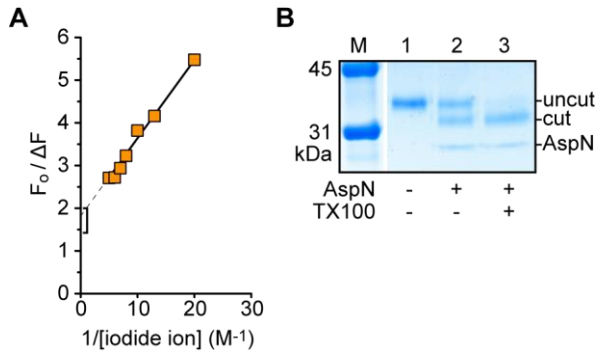
A. Absorbance spectra of RhoWT and RhoM257Y regenerated with 11-*cis*-retinal. ‘Dark’ spectra of both RhoWT (1) and RhoM257Y (3) recorded after purification had the expected absorption maximum at 500 nm. ‘Light’ spectra recorded after light-activation (>515 nm wavelength light for 60 s) of RhoWT in the presence of hydroxylamine (2) and RhoM257Y (Rho*, 4). Acidification of Rho* reveals the diagnostic absorption maximum red-shift for protonated Schiff-base linked all-*trans*-retinal (5).

B. Absorbance spectra, as in panel A, for RhoWT and RhoM257Y regenerated with 9-*cis*-retinal. As the structure of these isorhodopsins are virtually indistinguishable from that of rhodopsin¹, we have used 9-*cis*-retinal-containing isorhodopsins for scramblase analyses.

C. G_t activation was measured by the intrinsic G_t Trp fluorescence in the presence of catalytic amounts of immunopurified RhoWT (red trace), Rho* (orange trace) and bovine rod disc rhodopsin (Rho_{ros}, black trace). The baseline fluorescence was established after light exposure ($h\nu$), followed by addition of GTP γ S (arrow) to initiate the reaction. The reaction was monitored for 600 s before further addition of light-activated Rho_{ros}* (arrow) to activate the whole pool of G_t. The traces are vertically displaced by 0.1 relative intensity units for clarity.

D. G_t activation analysis as in **C**, but without exposing Rho* or RhoWT to light. Rho* was activated several hours before the assay. The data show that only Rho* is constitutively active, As RhoM257Y was light-activated to form Rho* several hours before the measurement, the G_t activation data show that Rho* retains its active conformation over the period of time necessary to perform the scramblase assay.

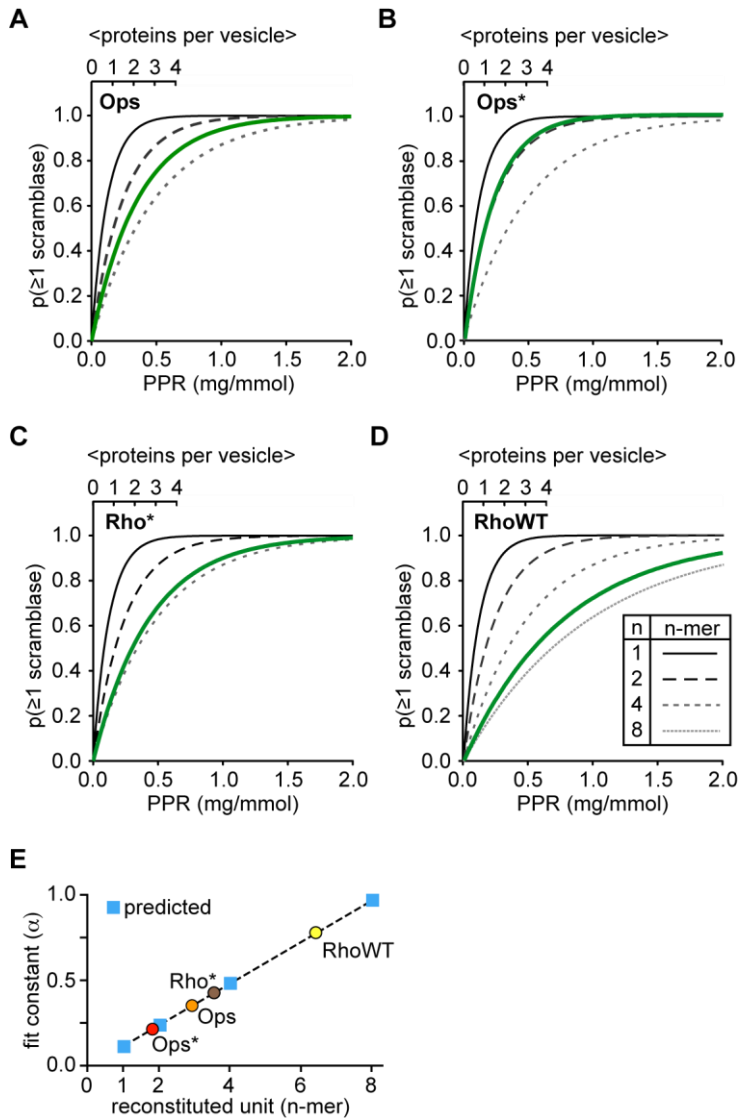
E. G_t activation by RhoWT (red), Rho* (orange) and Rho_{ros} (black) was performed and analyzed as described in 'Supplementary Methods' for the indicated concentrations. The resulting values are 5.86 ± 0.12 (Rho*), 5.60 ± 0.01 (RhoWT), and 5.73 ± 0.09 (Rho_{ros}) nM G_t activated per second per nM pigment. Error bars are \pm SD of the linear fit from the individual activation experiments. As observed previously, activation of G_t by Rho* was slightly higher than that for RhoWT ².



Supplementary Figure 2. NBD-phospholipids and opsin are symmetrically reconstituted.

A. NBD-PC-containing proteoliposomes were prepared by the destabilization method as described in ‘Methods’ at a protein/phospholipid ratio (PPR) of ~ 2.5 mg/mmol. Opsin purified from bovine discs was used for this experiment, and 250 mM KCl was used in place of 100 mM NaCl in the reconstitution buffer. Samples were taken for collisional quenching with iodide ions as described ³. The data were analyzed according to a modified Stern-Volmer equation ³. The inverse of the y-intercept to the graph represents the fraction of NBD-PC in the sample that is accessible to quenching by iodide ions. For the data shown, the intercept is 1.7 (95% confidence interval 1.4 to 2.0; square bracket), consistent with the expectation that NBD-PC is symmetrically distributed between the inner and outer leaflet of proteoliposomes. The collisional quenching results also constitute evidence that iodide ions cannot penetrate to the interior of opsin-containing vesicles.

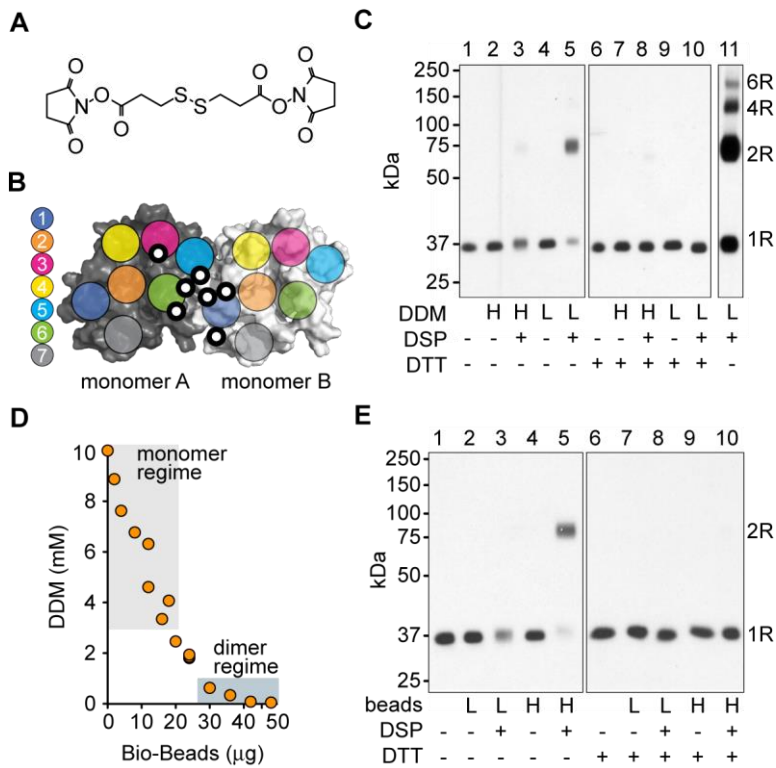
B. Opsin-proteoliposomes were prepared as described in ‘Methods’ at a PPR of ~ 2.5 mg/mmol, except that NBD-phospholipids were omitted. The vesicles were treated with a 2-fold molar excess of the endoproteinase AspN (NEB, Ipswich MA) for 60 min at room temperature (lane 2). As controls, the proteoliposomes were treated with AspN ⁴ in the presence of Triton X-100 to permeabilize the vesicles (lane 3), or mock-treated by omitting the protease (lane 1). Samples were analyzed by SDS-PAGE using a 10% gel, and visualized by Coomassie Blue staining. Bands were quantified by densitometry. AspN cleaved 44% of the reconstituted opsin in intact vesicles (lane 2) and 82% in disrupted vesicles (lane 3). Adjusting for the efficiency of cleavage in disrupted vesicles, $\sim 54\%$ of the opsin molecules were accessible to AspN in intact vesicles. In an independent experiment, 46% and 51% cleavage was observed after 30 and 60 min treatment, respectively. These results indicate that opsin is symmetrically reconstituted.



Supplementary Figure 3. Predicted plots of $p(\geq 1 \text{ scramblase})$ versus PPR for the reconstitution of monomers and multimers of Ops, Ops*, Rho* and RhoWT into unilamellar vesicles.

A-D. Graphs of $p(\geq 1 \text{ scramblase})$ versus PPR were generated for the reconstitution of multimers (n-mers, with $n=1,2,4$ and 8) of Ops, Ops*, Rho* and RhoWT into 200 nm diameter unilamellar vesicles. A sample calculation for the case of $n=1$ is presented in ‘Methods’. The upper x-axis indicates PPR values converted to the average number of monomers per vesicle. The green lines are taken from Figure 3A, C and D and Figure 4C.

E. Graph of the fit constant α for the equation $p(\geq 1 \text{ scramblase}) = 1 - \exp(-\text{PPR}/\alpha)$ as a function of the size of the multimer being reconstituted (n-mer). Predicted values for the reconstitution of opsin monomers, dimers, tetramers and octamers are shown as blue squares (the dashed line connecting the squares is intended to guide the eye). Measured fit constants for Ops, Ops* and Rho* (taken from the data in Fig. 3 panels A, C and D) and RhoWT (taken from data in Fig. 4 panel C) are indicated.



Supplementary Figure 4. Cross-linking reactions reveal that the oligomeric state of rhodopsin is sensitive to protein:detergent ratio.

These chemical cross-linking studies support our hypothesis that whereas rhodopsin is monomeric when fully solubilized in DDM, it dimerizes (and potentially multimerizes) when the detergent concentration is reduced as would be required for reconstitution of the protein into vesicles. This result explains why rhodopsin inserts into vesicles as a pre-formed higher order structure rather than as a monomer. Although similar studies in proteoliposomes were inconclusive due to the presence of DTT- and SDS-resistant aggregation of rhodopsin under the experimental conditions, it has been demonstrated previously using fluorescence-based analyses (FRET/LRET) that rhodopsin in proteoliposomes exists as a multimer⁵.

A. Structure of dithiobis[succinimidyl propionate] (DSP), a homobifunctional, amine-reactive cross-linking reagent with a 1.2 nm spacer arm containing a disulfide bond that can be cleaved with dithiothreitol (DTT).

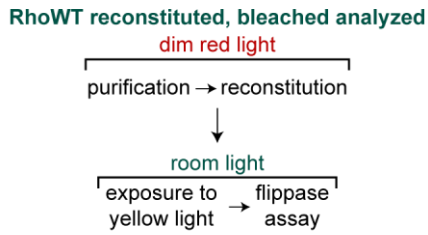
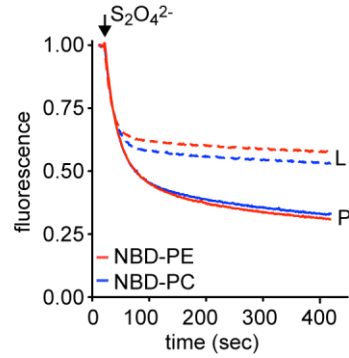
B. A cytosol-facing surface visualization of a proposed rhodopsin dimer interface overlaid with color-coded circles representing the transmembrane helices and thickly outlined white circles representing reactive lysines. DSP is predicted to cross-link monomers within a rhodopsin dimer by reacting with Lys141, Lys231, Lys245, and Lys248 on rhodopsin monomer A, and Lys66, Lys67 and Lys339 on rhodopsin monomer B. Adapted from⁶.

C. Western blot of rhodopsin from bovine disc membranes (Rho_{ros}) solubilized at 10 mM DDM (H, ~900-fold molar excess) or 0.2 mM DDM (L, ~20-fold molar excess) cross-linked with 125-fold molar excess of DSP. Rho_{ros} was used for these studies rather than the rhodopsin and opsin constructs that we expressed in COS-7 cells as the latter proteins are heterogeneously *N*-glycosylated making crosslinking difficult to assess by SDS-PAGE analysis. Untreated ROS

membranes, DSP-treated and mock-treated solubilized membranes as indicated were analyzed by either non-reducing (lanes 1-5) or reducing (lanes 6-10) SDS-PAGE. No cross-linking was observed in discs treated with high DDM treatment (lane 3), consistent with the expectation that fully solubilized rhodopsin is monomeric. However, in low DDM, DSP treatment resulted in the production of DTT-sensitive cross-linked rhodopsin dimers (lanes 5 vs. 10). While the samples were loaded onto a single gel, intervening lanes have been removed for clarity. Lane 11 is a 10-fold longer exposure of lane 5 revealing higher order oligomers. The expected mobility of monomeric, dimeric, tetrameric and hexameric rhodopsins is indicated on the right.

D. Adsorption of DDM by Bio-beads. Bio-beads, as indicated, were added to 200 μ L of 10 mM DDM in Buffer A and incubated with end-over-end mixing for 1 hour at RT. Detergent recovery was quantified as described in 'Methods'. Shaded boxes indicate the regimes that support monomers and dimers as described in ⁶.

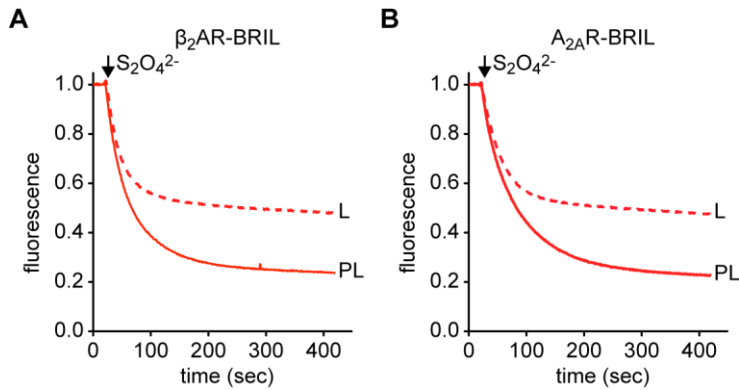
E. Detergent withdrawal induces formation of rhodopsin dimers as revealed by DSP cross-linking. ROS membranes were solubilized in Buffer A with 10 mM DDM and treated with either 5 (L) or 26.5 (H) μ g of bio-beads for 1 hour with mixing at RT. Untreated ROS membranes, DSP-treated and mock-treated solubilized and bead-treated membranes, as indicated, were analyzed by western blot after non-reducing (lanes 1-5) or reducing (lanes 6-10) SDS-PAGE. No cross-linking was observed in the sample treated with 5 μ g Bio-beads, i.e. a sample containing \sim 8 mM DDM, but a DTT-sensitive dimer band was quantitatively generated in the sample treated with 26.5 μ g Bio-beads that contained <1 mM DDM (lanes 3 vs. 5, and 5 vs. 10). The expected mobility of monomeric and dimeric rhodopsin is indicated on the right.

A**B**

Supplementary Figure 5. Scramblase activity of proteoliposomes reconstituted with RhoWT under dim red light and exposed to yellow light prior to assay.

A. Experimental protocol. RhoWT was purified and reconstituted into proteoliposomes (PPR ~1.2 mg/mmol) containing either NBD-PC or NBD-PE, all under dim red light. The sample was exposed to yellow light before being taken for scramblase activity assay.

B. Fluorescence reduction traces obtained by adding dithionite ($S_2O_4^{2-}$) at $t = 10$ s to RhoWT-proteoliposomes. Experimental details are as described for Figure 3B-D.



Supplementary Figure 6. Scramblase activity of β_2 AR-BRIL and A_{2A} AR-BRIL.

These data demonstrate that other rhodopsin-like GPCRs can scramble lipids. The constructs were purified and tested in the presence of their respective high affinity antagonists to ensure protein stability. It was not possible to assay ligand-free receptors under our experimental conditions.

A. Fluorescence reduction traces obtained by adding dithionite ($S_2O_4^{2-}$) at $t = 20$ s to proteoliposomes (PL) containing β_2 AR-BRIL (PPR 1.15 mg/mmol) reconstituted as described in the ‘Supplementary Methods’ except that 100 μ M carazolol and 0.02 mol% CHS were included. Protein-free liposomes (L) were generated under the same conditions and assayed in parallel. NBD-PE was used as the reporter in both reconstitutions.

B. As in **A** but for A_{2A} AR-BRIL (PPR 1.15 mg/mmol) reconstituted as described in the ‘Supplementary Methods’ except that 100 μ M ZM-241385 and 0.02 mol% CHS were included.

Supplementary Methods

Spectroscopic characterization and quantification of rhodopsin and opsin

Spectral characterizations of RhoWT and Rho* were performed as previously reported ^{2,7}. Briefly, 25 μL of regenerated protein was diluted to 100 μL in 50 mM HEPES pH 7.4, 100 mM NaCl and 1.96 mM DDM in a semi-micro cuvette and 'dark' spectra were recorded in a Perkin-Elmer Lambda 800 UV-vis spectrophotometer. 'Light' spectra were recorded after exposing regenerated samples to yellow light (>515 nm) for 60 s. To ensure complete hydrolysis of the Schiff-base linkage to retinal, RhoWT samples were also treated with 50 mM NH_2OH . The Schiff-base linkage to all-*trans*-retinal in Rho* was confirmed by the diagnostic red-shift in the absorbance (from 380 nm to 440 nm) after addition of 2 μL of 5 M HCl to the cuvette. The concentration of RhoWT (11-*cis*-retinal or 9-*cis*-retinal) was determined from the dark/light difference intensity of the 500 nm or 484 nm peak using $\epsilon_{500}=42,700$ $\text{M}^{-1}\text{cm}^{-1}$ (Ref ⁸) or $\epsilon_{484}=43,200$ $\text{M}^{-1}\text{cm}^{-1}$ (Ref ⁹), respectively. In order to quantify non-regenerated opsins by SDS-PAGE, a correction factor was determined by using densitometry and Image J software ¹⁰ to compare spectrally quantified rhodopsins to the same samples quantified against an in-gel bovine serum albumin standard by SDS-PAGE and Coomassie staining.

G protein activation assays

G protein activation was measured by monitoring the change in transducin (G_t) tryptophan fluorescence essentially as described previously using a SPEX Fluorolog 3 spectrofluorometer ¹¹. The experimental protocol was slightly modified as follows. Briefly, 0.25 - 2.5 nM RhoWT, Rho* or native rhodopsin purified from bovine rod discs (Rho_{ROS}) were brought to 850 μL containing 750 nM G_t , 2 mM DTT, 130 mM NaCl, 1 mM MgCl_2 , 20 mM BTP pH 7.1 and 0.118 mM DDM. The samples were added to a fluorescence cuvette with constant stirring and equilibrated at 15°C for 4 min. For 'dark' measurements, the assay was initiated by adding 200 μM $\text{GTP}\gamma\text{S}$ after establishing the baseline fluorescence for 60 s (excitation 300 nm, emission 345 nm). After 600 s the whole pool of transducin was activated by addition of 200 nM purified light-activated $\text{Rho}_{\text{ROS}}^*$ to the reaction. 'Light' measurements were performed similarly, except that $\text{GTP}\gamma\text{S}$ was added 80 s after illumination with yellow light for 60 s. The data were analyzed as previously described ¹¹.

Cross-linking experiments

The procedure for cross-linking rhodopsin with DSP was adapted from a previous report ⁶. All steps prior to SDS-PAGE were performed under dim red light. To reproduce previously published results, ROS disc membranes were solubilized in Buffer A (50 mM HEPES pH 7.4, 100 mM NaCl) such that the final concentrations of protein and DDM were 0.4 mg/mL (rhodopsin) and either 10 mM or 0.2 mM (DDM) as indicated, and incubated for 1 hour on ice. The solubilized ROS membranes were reacted for 30 min on ice with a 125-fold molar excess of DSP (50 mM in DMSO) before quenching the reaction with 100 mM Tris-HCl pH 7.4. Control experiments included DMSO. DSP cross-linked reactions were further incubated on ice for 25 minutes with or without 150 mM dithiothreitol. To evaluate cross-linking after detergent withdrawal, ROS membranes were solubilized in 200 μL of 10 mM DDM, as described above, and then incubated with the indicated weight of Bio-beads prior to adding DSP. The detergent adsorption capacity of Bio-beads was determined by quantifying residual DDM ¹² in samples of 200 μL 10 mM DDM in Buffer A that were incubated with Bio-beads (quantity as indicated) for 1 hour at RT with mixing.

The cross-linking reactions were visualized by SDS-PAGE and western blotting using monoclonal anti-1D4 antibodies directed against rhodopsin in conjunction with anti-mouse IgG HRP conjugate.

β_2 AR and A_{2A} AR reconstitution and scramblase assays

β_2 -adrenergic receptor (β_2 AR-BRIL) and adenosine A_{2A} receptor (A_{2A} AR-BRIL) were expressed and purified as apocytochrome b562RIL fusions as previously described¹³. Both preparations were purified in 0.98 mM DDM / 0.01% cholesteryl hemisuccinate (CHS) and 100 μ M of antagonists carazolol or ZM 241385, respectively (the antagonists were included for protein stability). For proteoliposome reconstitution, 800 μ L of liposomes, prepared as described in 'Methods' were first destabilized in an 840 μ L reaction containing 8.09 mM DDM and 0.024% CHS. After incubation for 3 hours at RT with end-over-end mixing, NBD-phospholipids, DDM-solubilized receptor and the appropriate antagonist in DMSO were added to bring the final 1 mL reaction to 7 mM DDM, 0.02% CHS and 100 μ M antagonist. Bio-beads were then added as described in 'Methods' to remove detergent and enable vesicle reconstitution. Control liposomes with antagonist or DMSO were reconstituted in parallel. Samples were analyzed for lipid scrambling as described in 'Methods'.

Supplementary References

1. Nakamichi, H., Buss, V. & Okada, T. Photoisomerization mechanism of rhodopsin and 9-cis-rhodopsin revealed by x-ray crystallography. *Biophys J* **92**, L106–8 (2007).
2. Deupi, X. *et al.* Stabilized G protein binding site in the structure of constitutively active metarhodopsin-II. *Proc Natl Acad Sci U A* **109**, 119–24 (2012).
3. Vehring, S. *et al.* Flip-flop of fluorescently labeled phospholipids in proteoliposomes reconstituted with *Saccharomyces cerevisiae* microsomal proteins. *Eukaryot Cell* **6**, 1625–34 (2007).
4. Niu, L., Kim, J. M. & Khorana, H. G. Structure and function in rhodopsin: asymmetric reconstitution of rhodopsin in liposomes. *Proc Natl Acad Sci U A* **99**, 13409–12 (2002).
5. Mansoor, S. E., Palczewski, K. & Farrens, D. L. Rhodopsin self-associates in asolectin liposomes. *Proc Natl Acad Sci U A* **103**, 3060–5 (2006).
6. Jastrzebska, B. *et al.* Functional characterization of rhodopsin monomers and dimers in detergents. *J Biol Chem* **279**, 54663–75 (2004).
7. Xie, G., Gross, A. K. & Oprian, D. D. An opsin mutant with increased thermal stability. *Biochemistry* **42**, 1995–2001 (2003).
8. Franke, R. R., Sakmar, T. P., Graham, R. M. & Khorana, H. G. Structure and function in rhodopsin. Studies of the interaction between the rhodopsin cytoplasmic domain and transducin. *J Biol Chem* **267**, 14767–74 (1992).
9. Toledo, D. *et al.* Molecular mechanisms of disease for mutations at Gly-90 in rhodopsin. *J Biol Chem* **286**, 39993–40001 (2011).
10. Schneider, C. A., Rasband, W. S. & Eliceiri, K. W. NIH Image to ImageJ: 25 years of image analysis. *Nat Methods* **9**, 671–5 (2012).
11. Ernst, O. P., Gramse, V., Kolbe, M., Hofmann, K. P. & Heck, M. Monomeric G protein-coupled receptor rhodopsin in solution activates its G protein transducin at the diffusion limit. *Proc Natl Acad Sci U A* **104**, 10859–64 (2007).
12. Urbani, A. & Warne, T. A colorimetric determination for glycosidic and bile salt-based detergents: applications in membrane protein research. *Anal Biochem* **336**, 117–24 (2005).
13. Chun, E. *et al.* Fusion partner toolchest for the stabilization and crystallization of G protein-coupled receptors. *Structure* **20**, 967–76 (2012).